

Prediction of Residual Stresses in Mild Steel Plate Weldments Using Intelligence Modelling Approach

^{1*}M. K. Achike, ²P. C. Onyechi and ³C. C. Ihueze

^{1*}*Department of Metalwork Technology Education, Federal College of Education (Technical), Umunze, Nigeria.*

^{2,3}*Department of Industrial and Production Engineering, Nnamdi Azikiwe University, Awka, Nigeria.*

Submitted: 01-09-2021

Revised: 09-09-2021

Accepted: 12-09-2021

ABSTRACT

This paper sought to determine the effects of welding parameters (current, voltage, welding speed and plate thickness) on the residual stresses induced on mild steel plate weldments obtained using Shielded Metal Arc Welding (SMAW) process. Taguchi method and intelligent modelling techniques (artificial neural networks and extreme learning machine) were used to analyze the experimental results obtained. In designing the experimental runs for this research, Taguchi design of experiment which consists of four controllable parameters at 3-levels of design for which we chose the $L_9(3^4)$ orthogonal array was used. Signal-to-noise ratio (S/N) was computed employing the smaller-the-better criterion for residual stress response using Minitab 17 Software and ANOVA was used to validate the results at 95% confidence level. The ANN and ELM model simulations were carried out in the MATLAB 2018a environment at three different hidden neural nodes of 10, 20 and 30 neurons for the thirty (30) experimental runs. ELM algorithm showed a very good model fit at 30 neural nodes with a coefficient of determination (R^2) value of 99.86% which is far better than that of ANN algorithm and regression model which has R^2 values of 96.52% and 92.61% respectively.

Keywords: Shielded Metal Arc Welding, Residual Stress, Taguchi Method, ANN and ELM

I. INTRODUCTION

Welding is one of the most important technologies widely used in various engineering fields such as civil engineering, shipbuilding, pipeline fabrication, steel structural fabrication among others. It is a complicated process accompanied by shrinkage effects, phase transformations, intensification of corrosion and arising of residual stresses. The American Welding

Society (2004) defined welding as a localized coalescence of metals or non-metals produced by either heating of the materials to a suitable temperature with or without the application of pressure, or by the application of pressure alone with or without the use of a filler material. It is a process that involves localized heat generation from a moving heat source. The welded structures are heated rapidly up to the melting temperature, and followed by rapid cooling which cause's micro-structural and property alteration. Arc welding processes use a welding power supply to create and maintain an electric arc between an electrode and the base material to melt metals at the welding point.

Many distinct factors influence the strength of welds and the material around them, including the welding method, the amount and concentration of energy input, the weldability of the base material, filler material, and flux material, the design of the joint, and the interactions between all these factors. To test the quality of a weld, either destructive or nondestructive testing methods are commonly used to verify that welds are free of defects, have acceptable levels of residual stresses and distortion, and have acceptable heat-affected zone (HAZ) properties.

Withers and Bhadeshia (2001) identify residual stress as the stress that remain within a material or body after manufacture and material processing in the absence of external forces or thermal gradients. Welding is one of the most significant causes of residual stresses and typically produces large tensile stresses in the weld, balanced by lower compressive residual stresses elsewhere in the component. Tensile residual stresses may reduce the performance or cause failure of manufactured products. They may increase the rate of damage by fatigue, creep or

environmental degradation. They may reduce the load carrying capacity of a component by contributing to failure by brittle fracture, or cause other forms of damage such as shape change or crazing (Bate, Green and Buttle, 1997; Masubichi, 1980).

Since residual stresses can affect structural behaviour, it is important to predict and model the residual stresses under different scenarios. Selection of appropriate welding parameters (current, voltage and welding speed) for a given material is essential in obtaining quality weld.

The principal material used in this research was AISI 1018 mild steel plate. Mild steel is especially desirable for construction due to its weldability and machinability. AISI 1018 mild steel has excellent weldability, produces a uniform

and harder case and it is considered the best steel for carburized parts (Jain, 2013). For each weldment, two plates of dimension 300×120×10mm, 300×120×8mm, and 300×120×6mm in each case were cut and welded to make a weld specimen plate of 300×240×10mm, 300×240×8mm and 300×240×6mm respectively with a 300 mm weld length. Prior to welding, the plates were cleaned from water, dust and oil to enable proper deposition of electrodes. The 60° single V-groove butt joint was used employing symmetric welding sequence and the plates were tack-welded at both ends in order to eliminate distortion during welding. All necessary precautions were taken to eliminate welding defects.

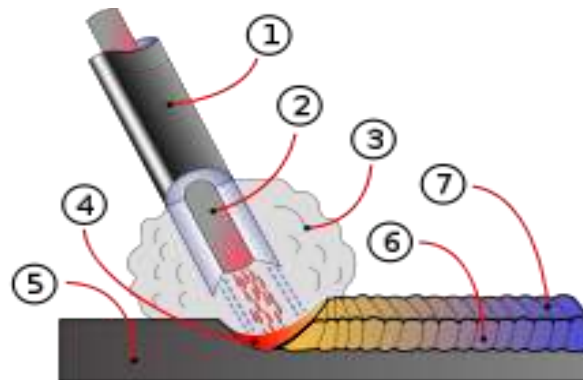


Figure 1: Shielded metal arc welding process

1. Coating flow 2. Rod 3. Shielding gas 4. Fusion 5. Base metal 6. Weld metal 7. Solidified slag

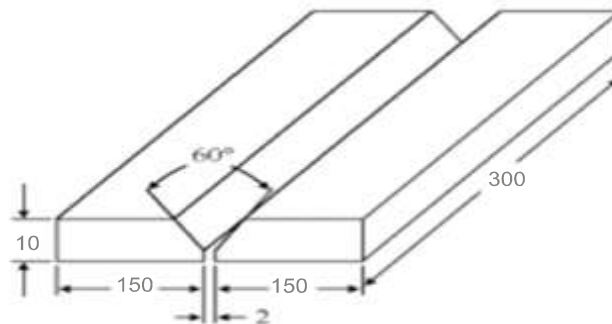


Figure 2: Plate set-up prior to welding

Experimental Design (Taguchi Method)

The modern day approach to find the optimal output over a set of given inputs can be easily carried out by the use of Taguchi method rather than using any other conventional method. The Taguchi method emphasizes the selection of the most optimal solution over the set of given inputs with a reduced cost and increased quality. The optimal solution so obtained is least affected

by any outside disturbances like the noise or any other environmental conditions (Rao et al., 2008). Okafor, Ihueze and Nwigbo (2013) viewed Taguchi robust design as a method of designing experiments in order to investigate how different parameters affect the mean and variance of a process performance characteristic that define how well the process is functioning.

The Taguchi method for design of experiment emphasizes the use of loss function, which is the deviation from the desired value of the quality characteristic. Based on this loss function, the Signal-to-Noise (S/N) ratio for each experimental run is evaluated and accordingly the optimal results are derived. S/N ratio is based upon the smaller-the-better criterion for residual stress which is given as:

$$\frac{S}{N} = -10 \log \frac{1}{n} \left(\sum y_i^2 \right) \quad (1)$$

Where n = number of measurements,
y_i = response value for each measurement.

Equally spaced three levels within the operating range of the process parameters were selected as presented in table 1. Based on Taguchi method, an L₉ (3⁴) Orthogonal Array (OA) which has nine different experiments was conducted and the result is shown in table 3.

Table 1: Process parameters, Codes, and Level values

Process Parameter	Code	Levels		
		1	2	3
Welding Current (A)	I	100	130	160
Welding Voltage (V)	V	24	28	32
Welding Speed (mm/min)	S	90	120	150
Plate Thickness (mm)	t	6	8	10

Residual Stress Measurement

X-ray diffraction (XRD) is a well-established, non-destructive method for the determination of residual stress in polycrystalline materials. 75% of companies and academics prefer to use XRD method in measuring residual stresses because the method is fast, can be repeatable, harmless to the specimen, and can control the specimen quality (Mazzolani, 2005). Residual stress induces small changes in the crystal lattice spacing of a material, which can be revealed by XRD with a very high sensitivity. From this, the lattice spacing in different directions and the related elastic strain can be determined. X-Ray Diffraction (XRD) was carried out on each of the samples in order to calculate the residual stress induced during welding. The ψ angles were tilted in steps of 9° in the range of 0° to 45°. The residual stress was estimated using the peak shift at ψ angles and d-spacing relationship of (211) plane.

The Young modulus (E) and Poisson's ratio (ν) of mild steel were taken as 210 GPa and 0.290 respectively in order to estimate the residual stress values. The residual stress (σ) was calculated by using equations (2) and (3) as derived by Cullity and Stock (2001).

$$\varepsilon = \frac{d - d_0}{d_0} \quad (2)$$

$$\sigma = \frac{E}{1 + \nu} \times \frac{1}{\sin^2 \psi} \times \varepsilon \quad (3)$$

Where d₀ is the strain free inter planer spacing, ε is the calculated strain and angle ψ is the angle between the surface normal and strain measurement direction. The change in inter planer space "d" due to residual stress was measured from XRD graphics as shown in figure 3 and tabulated in table 2.

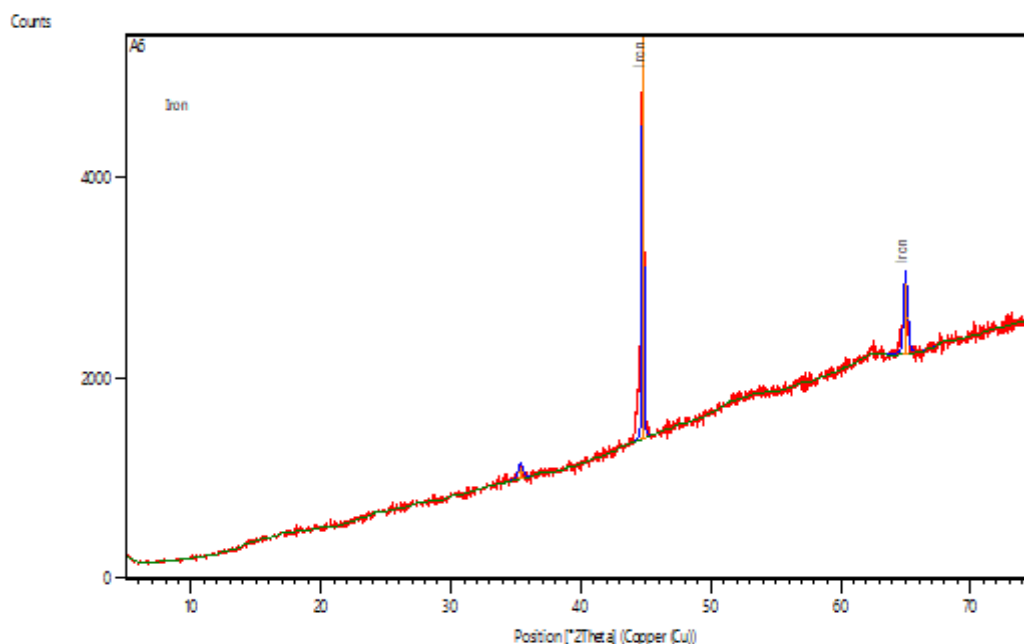


Figure 3: XRD Graphics

Table 2: Peak List

Pos.[°2Th.]	Height [cts]	FWHMLeft[°2Th.]	d-spacing [Å]	Rel. Int. [%]
35.3346	115.99	0.4093	2.54024	2.83
38.7350	204.21	0.0768	2.02587	10.00
44.9595	215.44	0.2558	1.43563	17.43
49.8367	99.08	0.6140	2.50580	14.69
55.2773	213.18	0.1279	2.00286	12.00
63.0348	181.53	0.6140	1.47475	8.59
65.4184	249.20	0.6140	1.42667	11.79
67.2773	113.18	0.1279	2.00286	16.24
68.0348	161.53	0.6140	1.47475	18.59

Experimental Results

The experimental result of residual stress (Table 3) was analyzed using Taguchi robust design. Minitab17 software was used for the Taguchi analysis which yielded the regression model for predicting residual stress response. The

response tables for signal-to-noise ratio and means (Table 4 and Table 5) for levels of each factor was obtained. The ranks based on delta statistics which compare the relative magnitude of effects were also analyzed.

Table 3: Experimental Result of Residual Stress

S/N	Input Variables				Response
	Current, I (A)	Voltage, V (V)	Welding Speed, S (mm/min)	Plate Thickness, t (mm)	Residual Stress (MPa)
1	100	24	90	6	272.4
2	100	28	120	8	186.6
3	100	32	150	10	142.0
4	130	24	120	10	265.4
5	130	28	150	6	220.6
6	130	32	90	8	318.5
7	160	24	150	8	260.8

8	160	28	90	10	325.2
9	160	32	120	6	312.8

Taguchi Analysis of Results

The experimental results were analyzed using Taguchi robust design and validated using ANOVA as a statistical tool. The results are shown in Tables 4 to 7.

Table 4: Response Table for Signal to Noise Ratio

	Welding			Plate
Level	Current (A)	Voltage (V)	Speed (mm/min)	Thickness (mm)
1	-45.32	-46.41	-48.21	-46.76
2	-46.71	-46.44	-46.59	-46.57
3	-47.95	-47.13	-45.18	-46.65
Delta	2.63	0.72	3.02	0.19
Rank	2	3	1	4

Table 5: Response Table for Means

	Welding			Plate
Level	Current (A)	Voltage (V)	Speed (mm/min)	Thickness (mm)
1	185.9	209.3	259.2	220.5
2	219.6	215.8	216.6	216.5
3	252.6	232.9	182.3	221.0
Delta	66.7	23.7	76.9	4.4
Rank	2	3	1	4

Table 6: Analysis of Variance for SN Ratio

Source	DF	Seq SS	Adj SS	Adj Ms	F	P
Current (A)	2	10.3592	10.3592	5.17961	1.82	0.015
Voltage (V)	2	0.9839	0.9839	0.49197	0.01	0.584
Welding Speed (mm/min)	2	13.7403	13.7403	6.87015	2.62	0.325
Plate Thickness(mm)	2	0.0554	0.0554	0.02772	0.00	0.112
Residual Error	2	1.0000				
Total	10	26.1389				

S = 0.3456 R² = 92.6% R² (Adj) = 42.4%

Table 7: Analysis of Variance for Means

Source	DF	Seq SS	Adj SS	Adj Ms	F	P
Current (A)	2	6673.6	6673.6	3336.81	35.05	0.235
Voltage (V)	2	895.6	895.6	447.82	8.62	0.015
Welding Speed (mm/min)	2	8904.3	8904.3	4452.15	21.40	0.522
Plate Thickness(mm)	2	35.8	35.8	17.92	2.46	0.204
Residual Error	2	0.0				
Total	10	16509.4				

S = 45.6486 R² = 90.2% R² (Adj) = 40.4%

The estimated model for S/N ratio is obtained as:

$$y = -46.6602 + 1.3376I - 0.0487I + 0.2496V + 0.2117V - 1.5457S + 0.0671S - 0.1025t + 0.0882t \quad (4)$$

The estimated model for Means is obtained as:

$$y = 219.344 - 33.478I + 0.256I - 10.078V - 3.511V + 39.822S - 2.744S + 1.189t - 2.811t \quad (5)$$

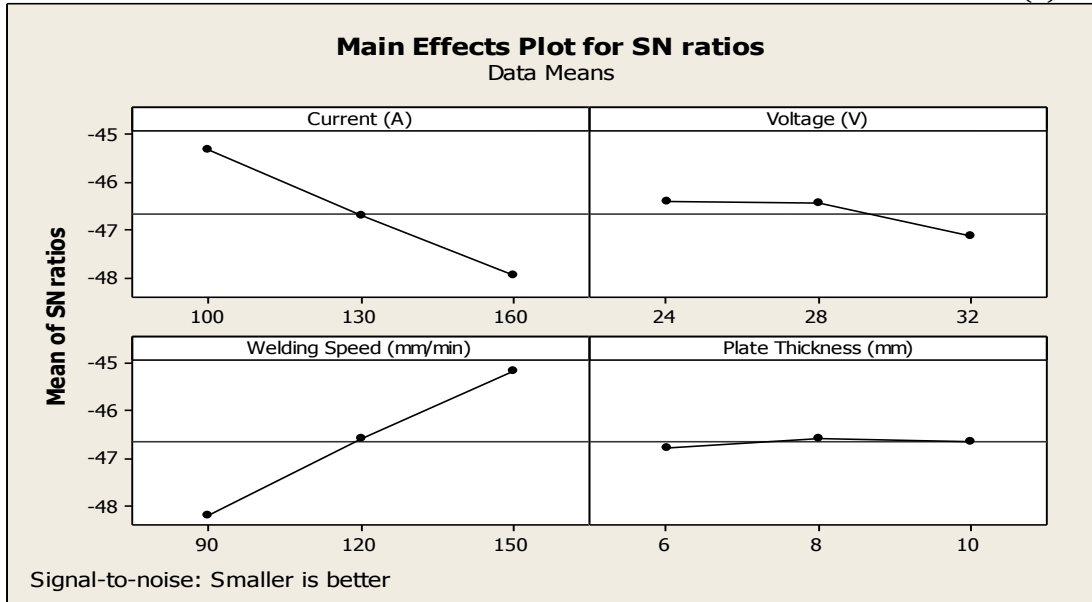


Figure 3: Main Effects Plot for SN Ratio

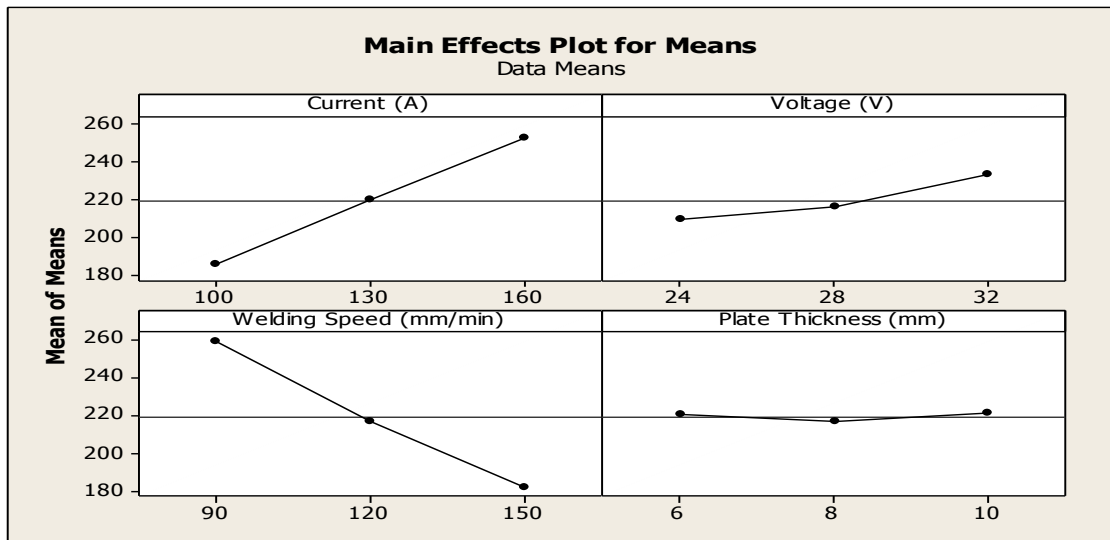


Figure 4: Main Effects Plot for Means

The response tables for signal-to-noise ratio and means for levels of each factor are shown in table 4 and table 5. The ranks in these response tables indicate that welding speed has the greatest influence on residual stress response of mild steel plate weldments obtained using shielded metal arc welding process. This was followed by welding current, welding voltage and plate thickness respectively.

In the analysis of variance, the coefficient of determination (R^2) at this point was 92.6% and 90.2% for S/N ratio and mean respectively. This

indicates that the linear models of S/N ratio and mean were able to show 92.6% and 90.2% of the variation observed in the dependent variable as captured by the explanatory variables in the linear regression model. These models were completely linear; they did not show interaction effects of the variables.

The main effects plots for S/N ratio and that of means (Figure 3 and 4) respectively indicate the same outcome of optimum. They show that the optimal residual stress for shielded metal arc welding was achieved at a welding current of

100A, welding voltage of 32V, welding speed of 150mm/min and plate thickness of 10mm.

The main effect plots, ranks of factors, values of sum of squares from ANOVA tables are all in conformity with coefficients of the linear models produced for this response. The absolute value of these coefficients shows the importance of each factor to the response; hence, welding speed remains the most significant factor. Based on equations (4) and (5), the optimal residual stress was obtained as 158.5MPa and 165MPa for S/N ratio and for means respectively.

ANN and ELM Modelling

The machine learning algorithms applied in this research are artificial neural networks (ANN) and extreme learning machine (ELM) which are both feed-forward neural networks. The ANN and ELM model simulations were carried out in MATLAB 2018a environment at three different hidden neural nodes of 10, 20 and 30 neurons for the thirty (30) experimental runs. The optimum ELM model was determined using the Sigmoid hidden transfer function while the optimum ANN model was determined using Levenberg-Marquart back propagation training algorithm.

The original dataset was split into training, cross-validation and test data sets, where;

- 70% of the exemplars were presented to the network for training.

$$MSE = \frac{1}{N} \sum_{i=1}^n (R_{Pi} - R_{Ti})^2 \quad (6)$$

$$RMSE = \sqrt{\frac{1}{N} \sum_{i=1}^n (R_{Pi} - R_{Ti})^2} \quad (7)$$

$$MAD = \frac{1}{N} \sum_{i=1}^n |(R_{Ti} - R_{Pi})| \quad (8)$$

$$MAPE = \frac{\sum (|R_T - R_P| / R_T) * 100}{N} \quad (9)$$

$$TS = \frac{\sum \frac{R_{Ti} - R_{Pi}}{R_{Ti}}}{\frac{1}{N} \sum_{i=1}^n |(R_{Ti} - R_{Pi})|} \quad (10)$$

$$R^2 = 1 - \frac{\sum_{i=0}^{n_{samples}} (R_{Ti} - R_{Pi})^2}{\sum_{i=0}^{n_{samples}} (R_{Ti} - \bar{R})^2} \quad (11)$$

Where R_{Pi} and R_{Ti} are the predicted and the targeted responses.

Table 8: Residual Stress Prediction Results

Experimental	ANN			ELM		
	10 Nodes	20 Nodes	30 Nodes	10 Nodes	20 Nodes	30 Nodes
265.4	268.54438	312.07867	288.17493	285.73168	272.70961	304.23639
325.2	362.13423	329.50677	361.6037	355.69669	331.12584	343.20903
318.5	376.71613	357.78855	351.39492	351.1324	327.94212	348.43963
220.6	234.71664	260.39327	225.17228	231.50884	231.38103	239.39717
312.8	334.23718	360.3945	334.57749	316.51783	319.91515	339.39047

- 15% of the exemplars concurrent with the training set were used for cross validation.
- 15% of the exemplars were used for testing the trained network.

The following termination criteria were used to determine convergence of the training algorithm:

- Number of runs before termination.
- Maximum number of runs.
- Non-improvement of cross-validation error with training.
- Increase in the cross-validation error with training.

Furthermore, a performance comparison in terms of estimation capacity was conducted between the two models to show their potential in predicting the response.

Score Metrics for ANN and ELM

To validate and compare the results from ANN and ELM models, the following score metrics were statistically evaluated. They are; Mean Square Error (MSE), Root Mean Square Error (RMSE), Mean Absolute Deviation (MAD), Mean Absolute Percentage Error (MAPE), Tracking Signal (TS) (Narasimhan, Mcleavey, and Billington, 1995; Vonderembse and White, 1991) and Coefficient of Determination (R^2) (Thorstom, 2017). These score metrics are expressed as follows;

Prediction Comparison of Residual Stress at 10, 20 and 30 Nodes

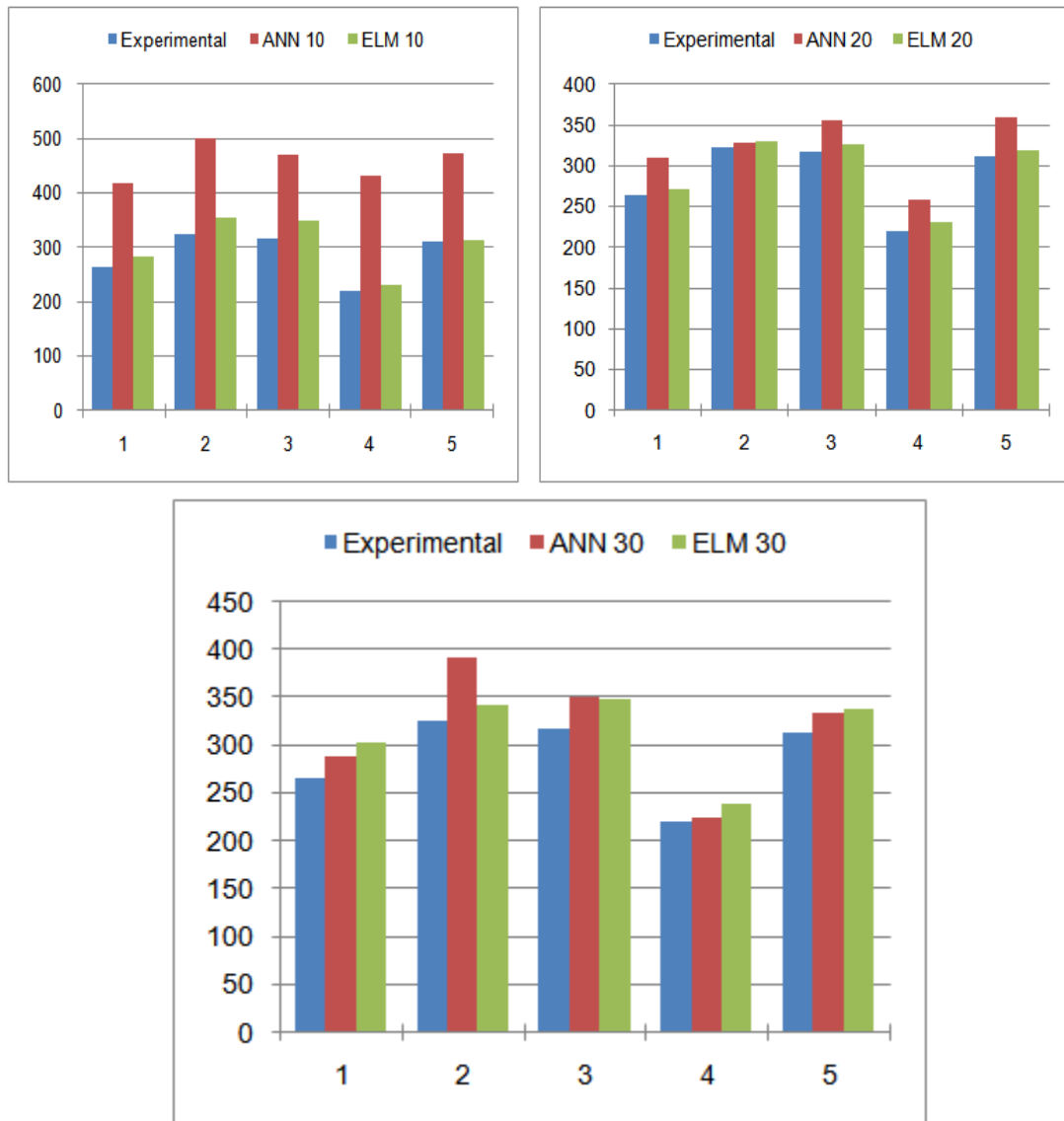


Figure 4: ANN and ELM Prediction Comparison of Residual Stress at 10, 20 and 30 Nodes

Figure 4 shows the graphical representation of the predicted values of residual stress response at 10, 20 and 30 nodes for both ANN and ELM models. It can be observed from the graphs that at node 30, ELM was the same as the expected values at all the measured points. The advantages of the ELM over the classical ANN model are evident. For example, in accordance with the basic theory of ELM, randomly initiated hidden neurons are fixed, and they do not need iterative tuning process with free parameters or connections

between hidden and output layer. Consequently, ELM is remarkably efficient to reach a global optimum, following universal approximation capability of single layer feed-forward network. With suitable activation functions, ELM can attain optimal generalization bounds of traditional feed forward neural networks in which all parameters are learned. This is a distinct advantage of the ELM model in terms of the efficiency and generalization performance over traditional learning algorithm such as ANN as revealed in this research.

ANN and ELM Scatter Plots for Residual Stress at 10, 20 and 30 Nodes

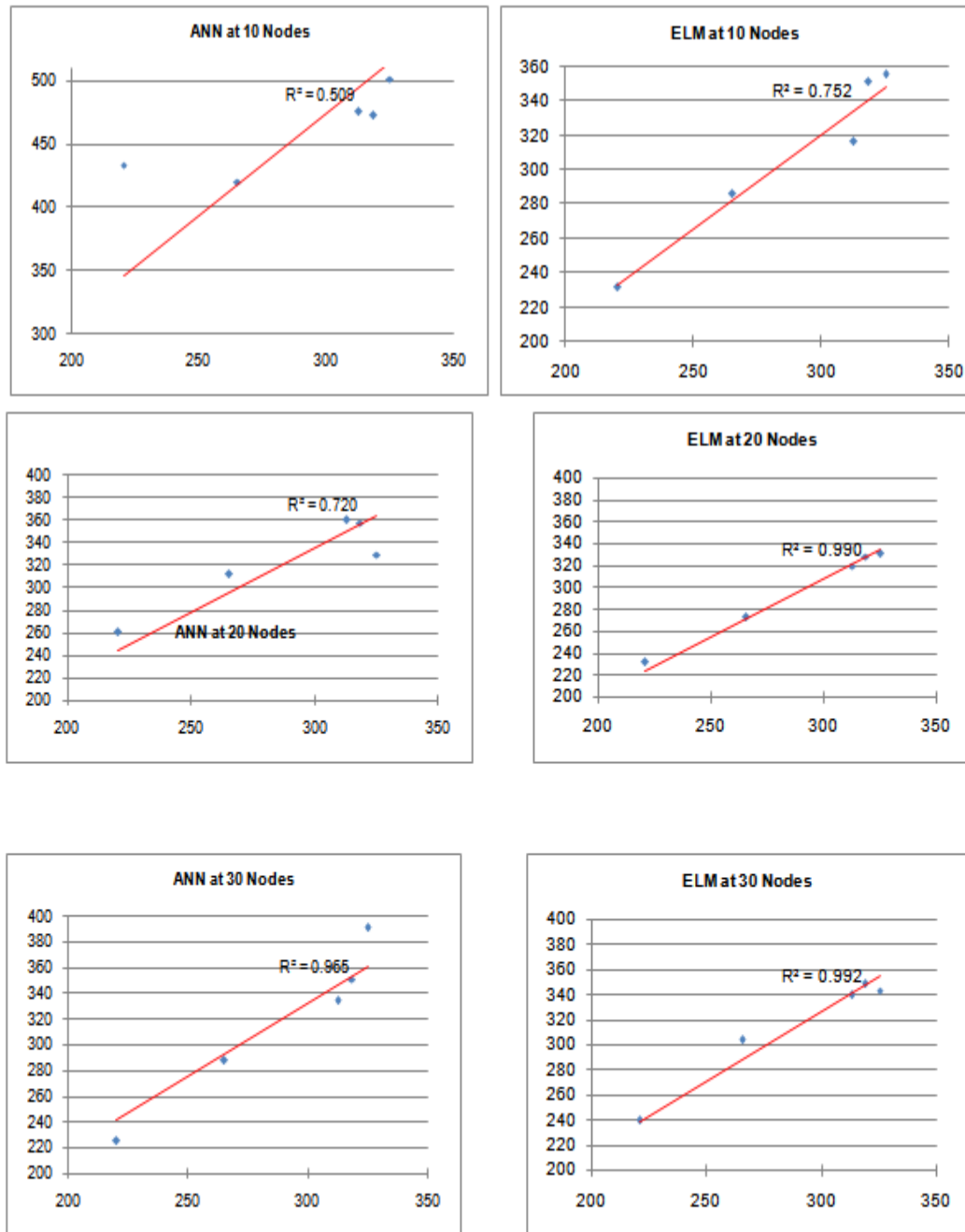


Figure 5: ANN and ELM Scatter Plots for Residual Stress Response at 10, 20 and 30 Nodes

Discussion of ANN and ELM Scatter Plots

The scatter plots of the predicted values at 10, 20 and 30 nodes are shown in figure 4. From the scatter plots, the highest degree of clusters at the linear regression line is clearly observed on the ELM model. This was specifically pronounced for the ELM model at 30 neural nodes. This particular statistical correlation of targeted and predicted

responses at optimum of 30 nodes has a coefficient of determination (R^2) value of 99.2% for ELM, 96.5% for ANN and 92.6% for Taguchi robust design. This result shows that ELM has better prediction capability compared to ANN.

The performance metrics for residual stress at 10, 20 and 30 nodes as obtained from equations (6) to (11) is shown in table 9.

Table 9: Performance Metrics for Residual Stress at 10, 20 and 30 Nodes

Metrics	ANN			ELM		
	10 Nodes	20 Nodes	30 Nodes	10 Nodes	20 Nodes	30 Nodes
MAD	143.28414	16.89536	19.30703	11.78426	5.02351	10.46137
MAPE	127.17983	16.31319	15.77781	9.84966	5.07485	10.18027
TS	-5	-5	-5	-5	-5	-5
R2	0.37293	0.64721	0.95199	0.93938	0.97432	0.62047
Time(s)	0.15784	0.08985	1.00246	0.00285	0.00089	0.00925
MSE	20954.24634	451.47165	483.50695	188.86352	50.02109	289.70185
RMSE	144.75582	21.24786	21.98879	13.74276	7.07256	17.02063

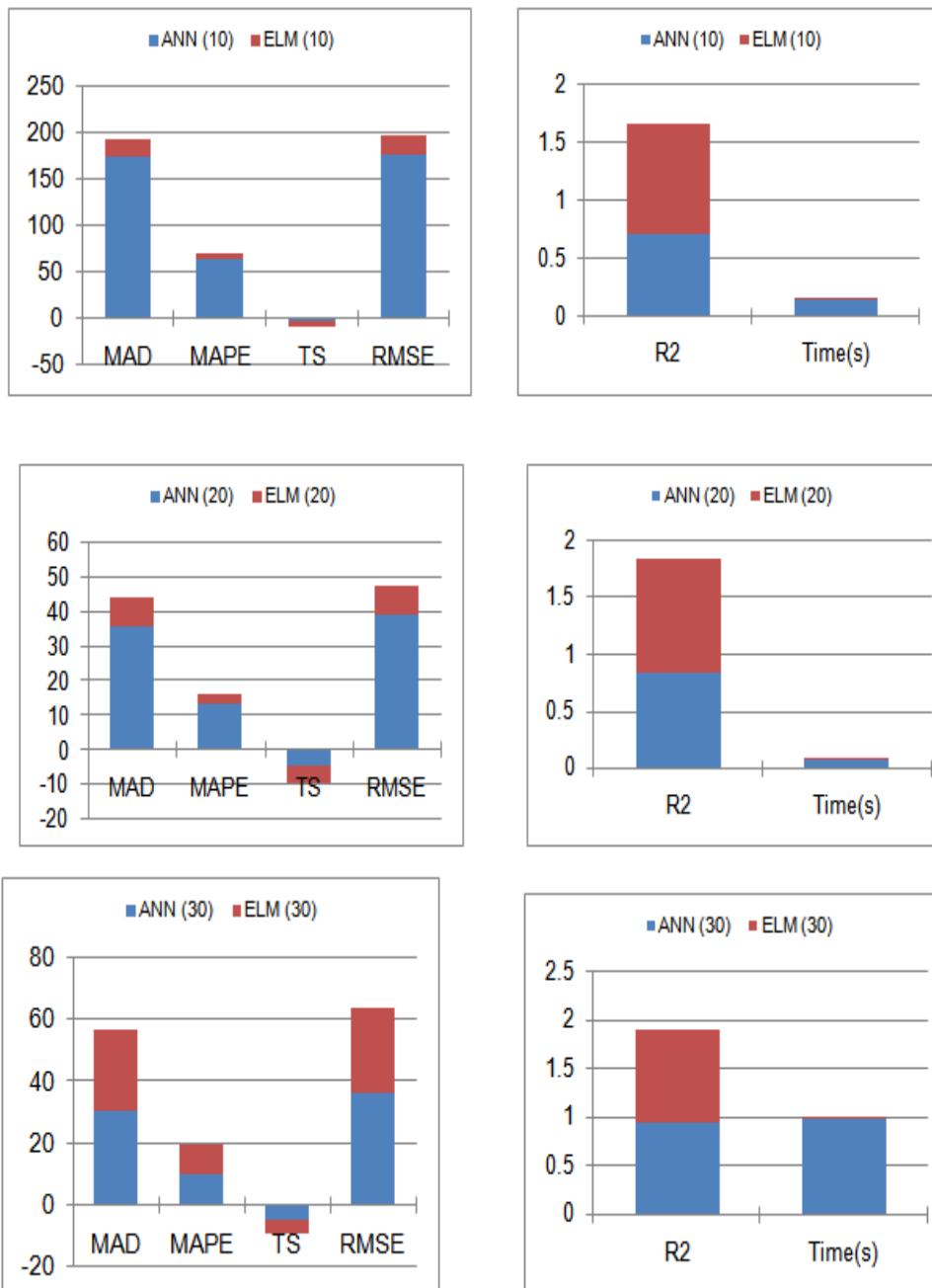


Figure 6: ANN and ELM Performance Metrics for Residual Stress at 10, 20 and 30 Nodes

From table 9, it is observed that ELM algorithm was simply magnificent in its training time which was much faster than that of ANN for all neural nodes. At 30 neural nodes, the training time for ELM was 0.009 Seconds while that of ANN was 1.00 Seconds.

The MSE and MAD are statistical approaches used to verify the prediction error. It was found that the MSE, RMSE, MAD and MAPE all improved as the output neuron value increased and fully converged at 30 neural nodes. This means that the higher the number of output neurons, the better the response. Comparing the two models, ELM attained full convergence at 20 output neurons while ANN was yet to attain its optimal response which was found to be at 30 nodes. The tracking signal (TS) helps to determine if the model is an accurate representation of the real-world variable. It is expected to be theoretically equal to zero. Both ELM and ANN models have tracking signals recorded at sub-zero for all the nodes. This indicates that the models have good tracking signal; hence the models are good.

II. CONCLUSIONS

At the end of this research, the following conclusions are made:

1. Based on analysis of the experimental results using Taguchi method, ANN and ELM algorithms, it can be concluded that all the methods gave reliable results.
2. Taguchi method can be successfully applied to analyze and optimize the parameters which influence the residual stresses on the weldments whereas ANN and ELM models can be used for predicting the response.
3. By comparing the experimental results with those obtained using ANN and ELM methods, it can be concluded that the ELM method is more efficient in prediction.

REFERENCES

- [1]. Bate, S.K., Green, D. and Buttle, D. (1997). A review of residual stress distribution in welded joints for defect assessment of offshore structures. *Journal of Material Manufacturing and Processing*, 4(5), 28-36.
- [2]. Cullity, B.D. and Stock, S.R. (2001). *Elements of X-ray diffraction*. 1st ed. New Jersey: Prentice Hall.
- [3]. Cynthia, L. and Annette, O. 2004. *The metallurgy of steel*. American Welding Society. (9th edition). ISBN 9780871708588.
- [4]. Jain, R. K., 2013. *Production Technology*. Khanna Publishers (17th edition), New Delhi.
- [5]. Masubichi K. (1980). *Analysis of Welded Structures: Residual Stresses, Distortions and their Consequences*, Pergamon Press, Oxford, UK.
- [6]. Mazzolani, T, Stone, H.J, Bhadeshia, H.K. and Withers, P.J. (2005). Characterizing phase transformations and their effects on ferritic weld residual stresses with X-rays and neutrons. *Metallurgy and Material Transaction*, 3(9), 3070–3078.
- [7]. Nasasimhan, J., Mcleavey, Z. and Billington, G., 1995. Composite function wavelength neural networks with extreme learning machine. *Journal of Neurocomputing*, 73(7), 1405-1416.
- [8]. Okafor, E.C., Ihueze, C. C. and Nwigbo, S.C., 2013. Optimization of hardness strengths response of plantain fibres reinforced polyester matrix composites applying Taguchi robust design. *International Journal of Engineering*, 26(1), 21-38.
- [9]. Rao, R.S., Ganesh, K.C., Shetty, P.S. and Phil, J.H., 2008. The Taguchi methodology as a statistical tool for biotechnological applications: A critical appraisal. *Biotechnology Journal*, 3(4), 510-523.
- [10]. Thorstom, H., 2017. Extreme learning machine and its applications. *Neural Computing and Applications*, 5, 14-34.
- [11]. Vonderembse, F. and White, T., 1991. Sales forecasting system based on gray Extreme Learning Machine with Taguchi method in retail industry. *Expert Systems with Applications*, 38(3), 1336-1345.
- [12]. Withers, P.J. and Bhadeshia, H.K. (2001). Residual stress: Part 1. *Journal of Material Science Technology*, 17, 355–365.